Royal Netherlands Meteorological Institute
Ministry of Infrastructure and the Environment

The EUMETSAT Network of Satellite Application Facilities

OSI SAF
Ocean and Sea Ice

EUMETSAT

Ocean and Sea Ice SAF

ASCAT/ERS higher order calibration

SAF/OSI/CDOP2/KNMI/TEC/RP/268

16 December 2016

Jeroen Verspeek

Ad Stoffelen

Royal Netherlands Meteorological Institute (KNMI)
De Bilt, the Netherlands

Summary

A new Geophysical Model Function (GMF) is being developed for C-band scatterometers. CMOD7 will be used for ERS and ASCAT wind retrievals and is valid for their combined incidence angle range. An intermediate GMF (CMOD6.2) is used as a starting point. For CMOD6.2 there exists a wind vector cell (WVC) dependency in the scatterometer wind speed probability distribution functions (pdf). Also local maxima arise in the wind speed pdf at wind speeds of 2 and 5 m/s.

A higher-order calibration (HOC) correction is applied for each WVC to match the scatterometer wind pdf to a predefined wind speed pdf. The predefined wind speed pdf is a combination of a theoretical function with fitted parameters on the ascending side, and a mean scatterometer pdf on the descending side. The HOC largely reduces the WVC-dependency of the wind speed pdf and also reduces the local maxima in the wind speed pdf.

Wind speed biases for the various scatterometer products, ERS-1, ASCAT-A and ASCAT-B (for 25 km WVC size and for the coastal product of 12.5 km WVC size) with respect to NWP stress-equivalent wind are compared to each other. NWP Ocean Calibration (NOC) is applied for ASCAT (using operational EWMF stress-equivalent winds) and for ERS (using ERA-interim stress-equivalent winds). Difference in bias caused by these differences in used NWP wind field and differences in the ECMWF software version, are compensated for.

The resulting CMOD7 shows good results on all relevant parameters, wind speed and direction, wind speed bias, cone distance and quality control rejection rate for both ERS and ASCAT scatterometers. Triple collocation with NWP and buoy winds also show good results.

Contents

1 Introduction

A new GMF is being developed for C-band scatterometers. CMOD7 will be used for ERS and ASCAT wind retrievals and is valid for their combined incidence angle range. Especially when reprocessing ERS and ASCAT in order to generate climatological data series a common GMF is useful in order to achieve consistent results. An intermediate GMF (named hereafter CMOD6.2) uses a combination of CMOD6 (See Verspeek, 2012) and C2013 (See Ricciardulli, 2014) and shows improvements in the retrieved wind distribution compared to CMOD6, especially for low winds. Still there remains a wind vector cell (WVC) dependency in the scatterometer wind speed probability distribution functions (pdf). Also local maxima arise in the wind speed pdf at wind speeds of 2 and 5 m/s (See Verspeek, 2015).

A higher-order calibration (HOC) correction is applied for each WVC to match the scatterometer wind pdf to a predefined wind speed pdf. The predefined wind speed pdf is a combination of a theoretical function with fitted parameters on the ascending side (for wind speeds below approximately 8 m/s), and a mean scatterometer pdf on the descending side (for wind speeds above approximately 8 m/s). See also Vogelzang and Stoffelen, 2016.

The HOC reduces the WVC-dependency of the wind speed pdf and also reduces the local maxima in the wind speed pdf.

In section 2 the HOC method is applied to ASCAT-A, yielding CMOD7.a. Wind statistics are subsequently shown. Then in section 3 the HOC method is applied to ERS-1, yielding CMOD7.e. Finally, CMOD7.a and CMOD7.e are combined into a consistent GMF for ERS and ASCAT, CMOD7.ae (or CMOD7) as described in section 4.

In section 5 the wind speed bias between scatterometer wind and NWP wind is examined. An inconsistency is present between NWP operational winds and NWP ERA-interim winds, which is eliminated with the help of NWP ocean calibration (NOC).

Finally in section 6 the statistics results from CMOD7 are discussed and in and section 7 the triple collocation method is used to validate CMOD7.

2 ASCAT higher order calibration

A higher-order calibration (HOC) correction is applied which matches the scatterometer wind pdf for each WVC to a predefined wind speed pdf. The predefined wind speed pdf is a combination of a theoretical function with fitted parameters on the ascending side, and a mean scatterometer pdf on the descending side (See Vogelzang and Stoffelen, 2016).

In Figure 1 and Figure 2 the HOC corrections ΔV are shown as a function of WVC and (uncorrected) wind speed. The corrections are quite symmetrical for left and right swath which means it may be expressed as a function of incidence angle instead of WVC. This is necessary for eventual incorporation in the GMF. Moreover, the fore and aft beam determine the wind speed retrieval to a large extent (e.g., Stoffelen and Anderson, 1997). Therefore, the mean fore and aft beam incidence angle at a WVC may be used to represent the GMF changes.

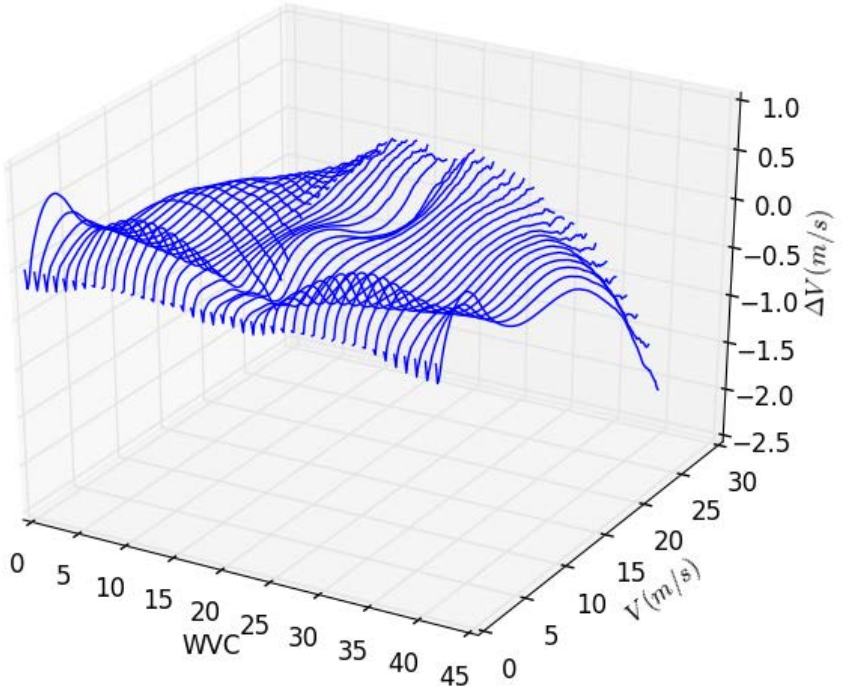

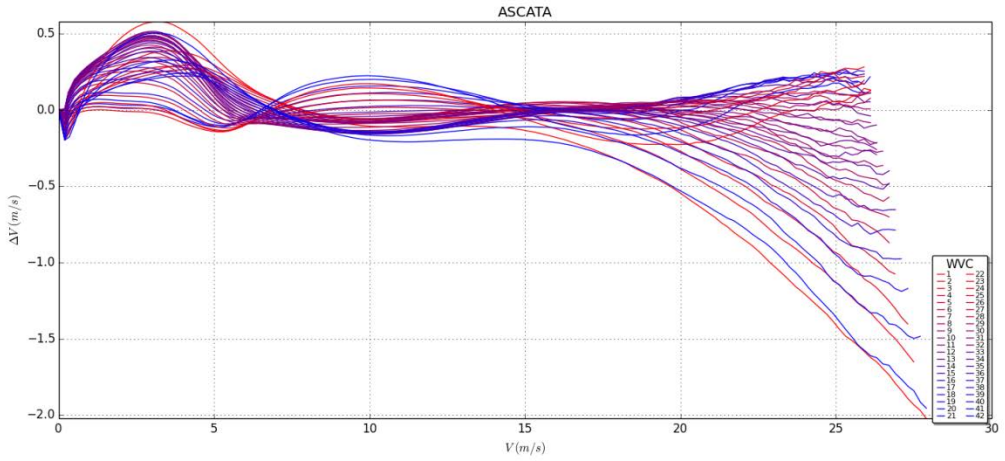

Figure 1 –higher order wind speed corrections from 2007/01 – 2014/03 ASCAT-A data

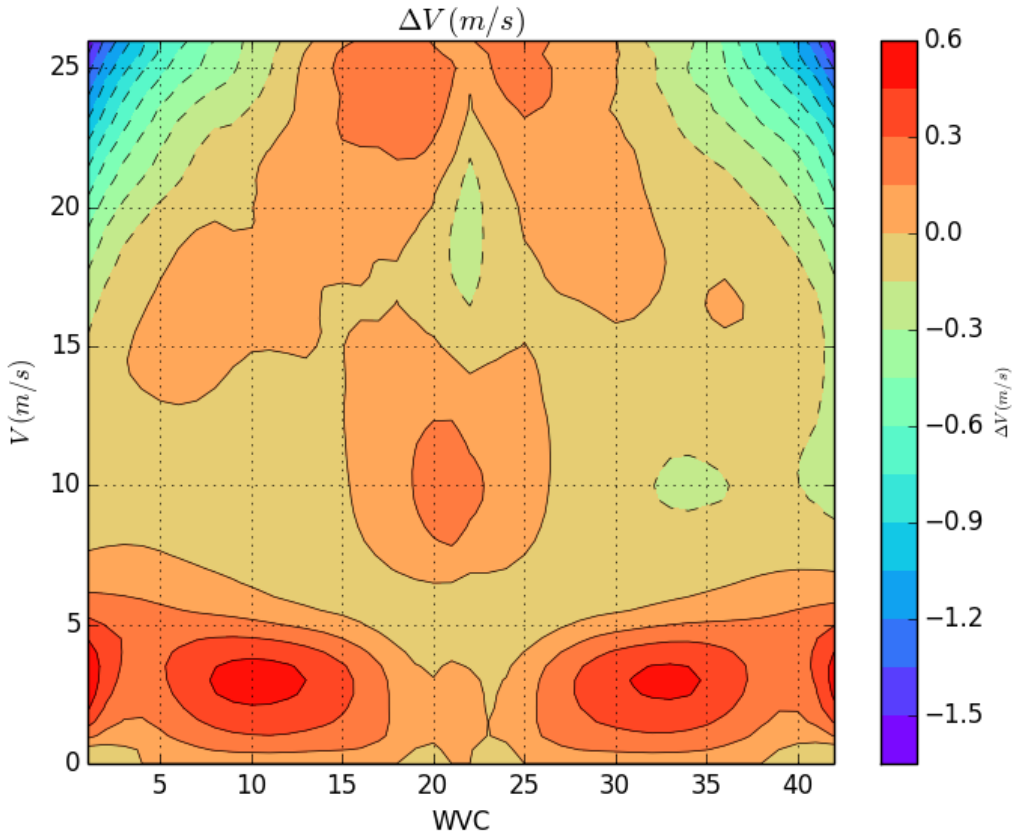

Figure 2 – wind speed correction as a function of wind speed and WVC based on ASCAT HOC

In Figure 3 the original ΔV per WVC is translated into ΔV per incidence angle by averaging corresponding left and right swath WVC ΔV corrections and fore and aft beam incidence angles. Then the ΔV is translated into a ΔB_0 with the aid of the GMF, i.e., the B_0 values at the modified and

original wind speeds are subtracted at each incidence angle. B_0 is defined as the GMF backscatter value averaged over the azimuth angle domain.

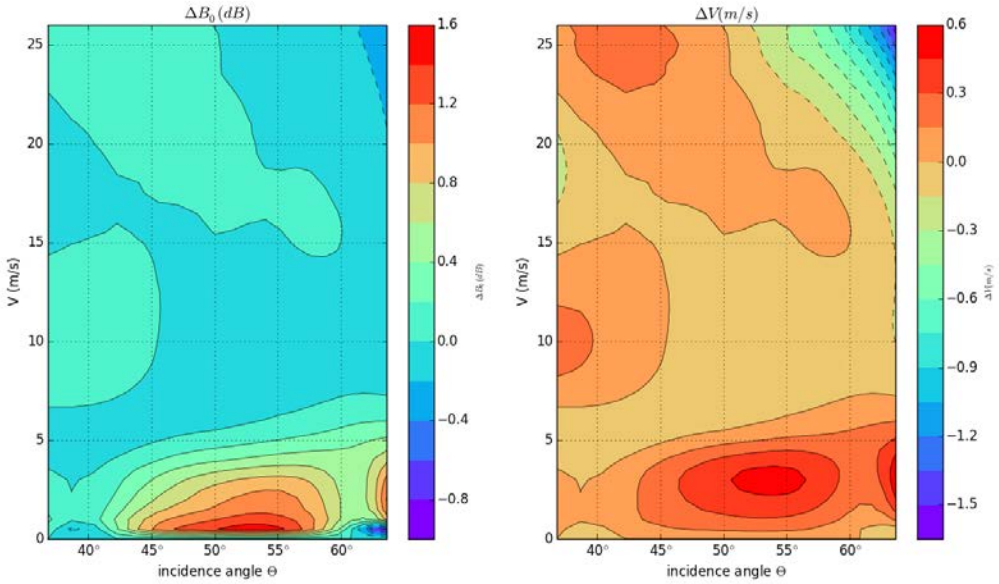

Figure 3– σ_0 correction (left) and wind speed correction (right) as a function of wind speed and incidence angle based on ASCAT HOC from the right swath only.

Finally, in Figure 4 the domain of the corrections is ad hoc extended and the binning size is adapted to the GMF look-up table (LUT) that is in use in AWDP, so that it may be applied in a HOC correction table. A LUT speed bin is selected with associated incidence angle and azimuth, ΔV is applied, and the backscatter and speed are written in an array for all wind speeds. Subsequently, the backscatter values are interpolated to the LUT speeds. This is repeated for all azimuth angles and incidence angles, resulting in a modified LUT.

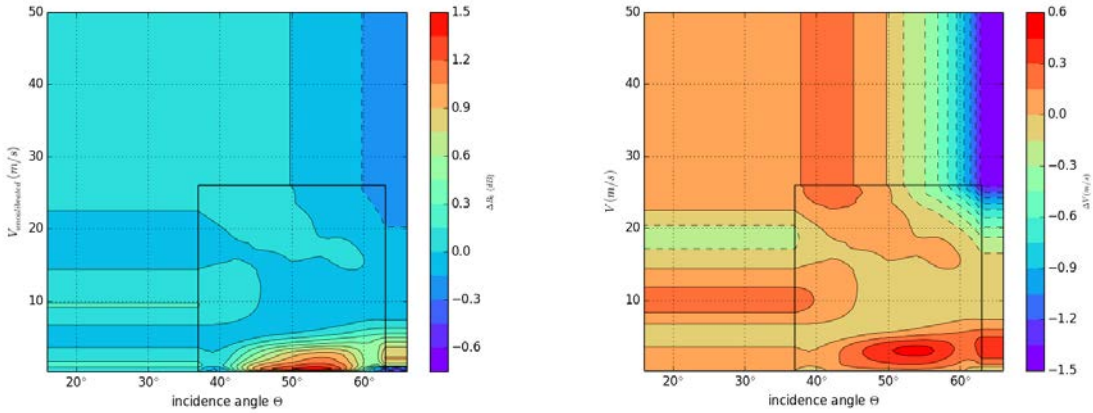

Figure 4 – σ_0 corrections (left) and wind speed correction (right) as a function of wind speed and incidence angle based on ASCAT HOC

Wind statistics (CMOD7.a)

In Figure 5 wind speed pdfs are shown from reprocessed ASCAT-A data of 2013-01 with stress-equivalent NWP winds from the ERA-interim ECWMF model.

In Figure 5a) the scatterometer wind pdf for the left and right swath are shown. The data is reprocessed with CMOD6.2 (without HOC correction). The artifacts for low winds that are present for CMOD5n are effectively eliminated by CMOD6.2. Still there is a WVC dependency of the wind speed pdfs which is most manifest at the top of the pdfs, but also in overall pdf shapes which tend to be narrower for low incidence angles.

In Figure 5b) the scatterometer wind pdf for the left and right swath are shown. The data is reprocessed with CMOD7 with HOC corrections from ASCAT-A (named CMOD7.a). The WVC dependency is largely reduced by the HOC corrections.

In Figure 5c) the NWP wind pdf for the left and right swath are shown.

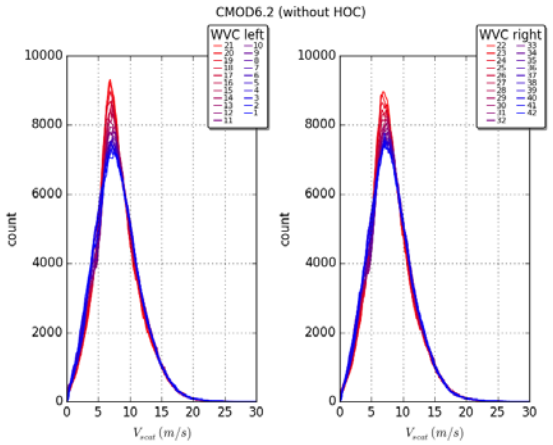

a)

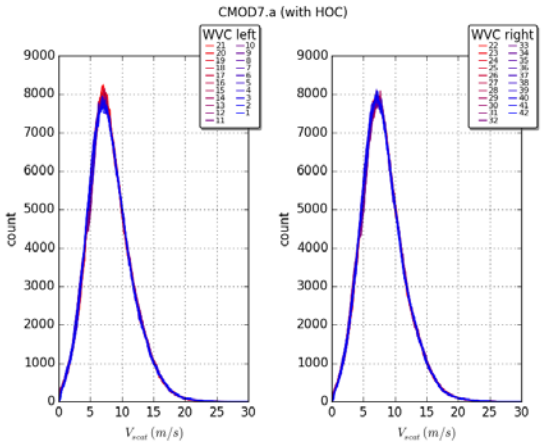

b)

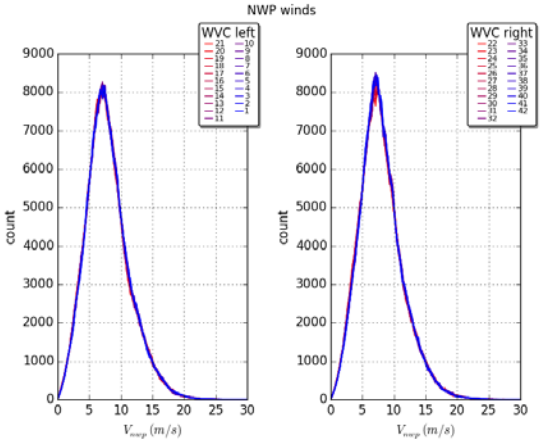

c)

Figure 5 – wind speed pdf from ASCAT-A left and right swath reprocessed data from 2013-01, ERA-interim stress equivalent winds

a) scattometer winds, CMOD6.2 (without HOC correction)

b) scattometer winds, CMOD7.a (with HOC correction)

c) ERA-interim stress-equivalent winds

In Figure 6 the wind speed and wind direction bias per WVC (scatterometer-ERA) are shown as well as their standard deviations.

Figure 6a) shows the biases for data reprocessed with CMOD6.2 (without HOC correction)

Figure 6b) show the biases for data reprocessed with CMOD7.a.

Wind speed biases do not vary much and the standard deviations show a slight improvement when HOC corrections are applied.

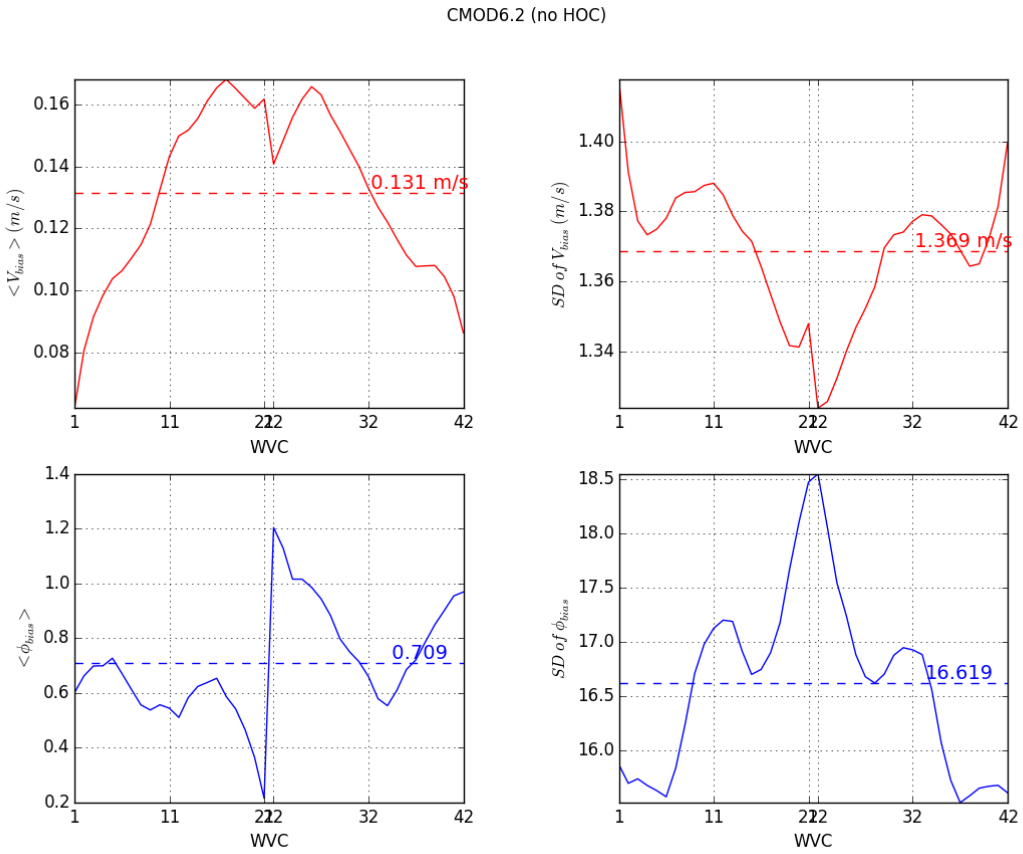

a)

CMOD7.a

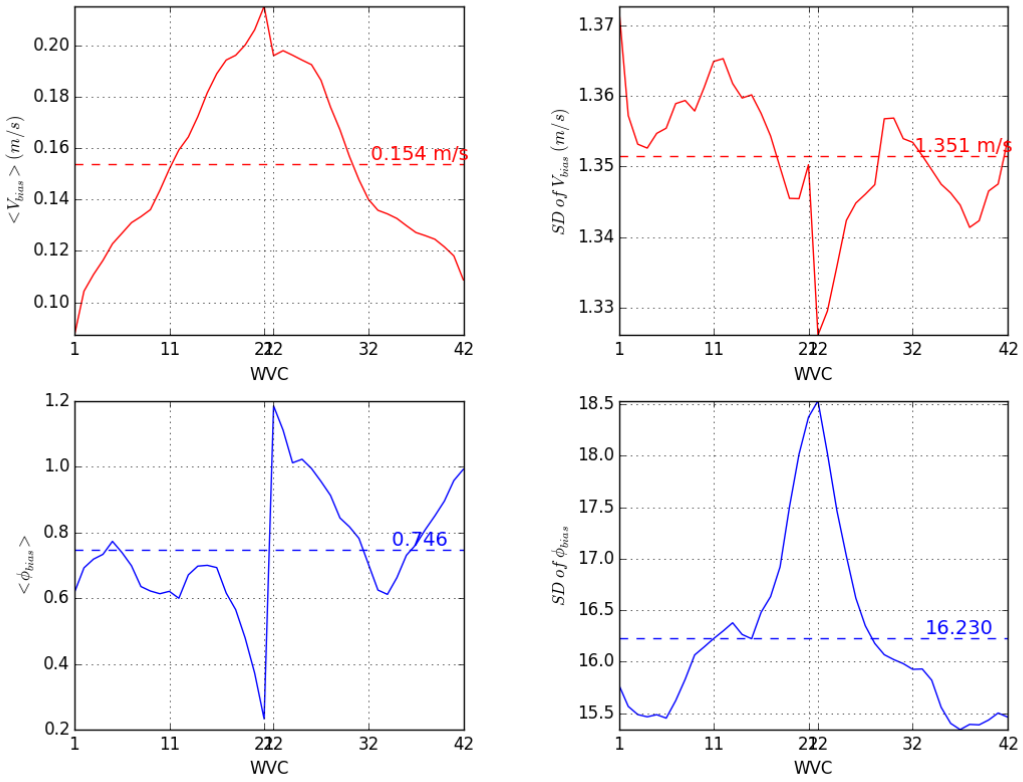

b)

Figure 6 – wind biases (scatterometer-NWP) per WVC for ASCAT-A reprocessed data from 2013-01, ERA-interim stress equivalent winds

a) CMOD6.2 (no HOC correction)

b) CMOD7.a

3 ERS higher-order calibration

Higher-order calibration (HOC) correction is applied to the ERS scatterometer data. The HOC is based on the incidence angles of the fore/aft beam only, as those beams are most important for determining the wind speed. For ASCAT this lowest fore and aft beam incidence angle is 37°, whereas for the ASCAT mid beam it is 27°. For ERS, the lowest fore and aft beam incidence angle is 25°, whereas for the ERS mid beam it is 18°. The ERS HOC could thus fill the gap between 27° and 37° for the incidence angle range of the ASCAT mid beam.

The ERS1 data of 1994 and 1995 are reprocessed with CMOD7.a (with the ASCAT HOC corrections included).

In Figure 7 the ERS-1 HOC corrections are shown, for the lower ERS incidence angles there are still large deviations, but for the higher incidence angles, the ASCAT HOC has indeed led to rather uniform wind speeds pdfs.

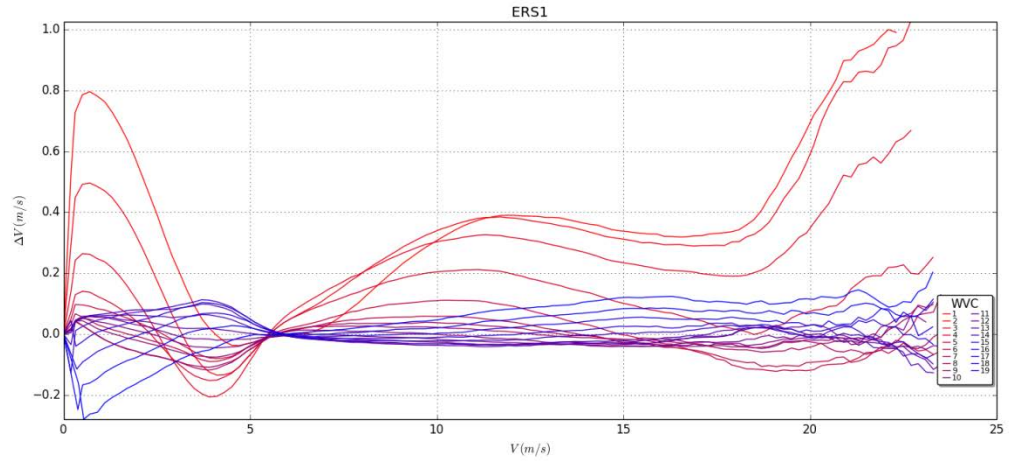
ERS1
1.0
0.8
0.6
0.4
0.2
0.0
−0.2
$\Delta V(m/s)$
0
5
10
15
20
25
$V(m/s)$
WVC
1
2
3
4
5
6
7
8
9
10
11
12
13
14
15
16
17
18
19

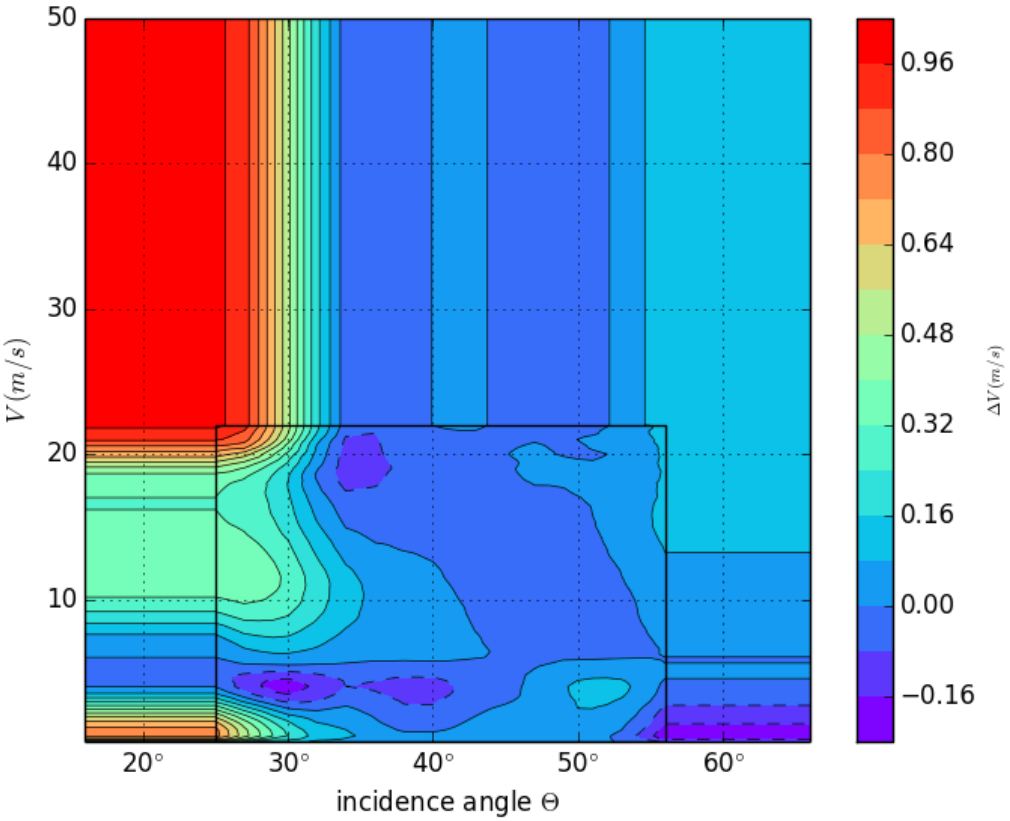
50
40
30
20
10
$V(m/s)$
20°
30°
40°
50°
60°
incidence angle Θ
0.96
0.80
0.64
0.48
0.32
0.16
0.00
−0.16
$\Delta V(m/s)$

Figure 7 – HOC corrections from ERS1 data of 1994 and 1995, reprocessed with CMOD7.a (with ASCAT HOC corrections).

Wind statistics (CMOD7.e)

In Figure 8 wind speed pdfs are shown from reprocessed ERS-1 data of 1995-01 with stress-equivalent NWP winds.

In Figure 8a) the ERS-1 scatterometer wind pdfs are shown. The data is reprocessed with CMOD7.a (with HOC corrections from ASCAT). Outer swath WVCs overlapping with the ASCAT incidence angles appear consistent, which is encouraging. In the inner swath, there is a WVC dependency of the wind speed as well as artefacts for low wind speed and low incidence angles.

In Figure 8b) also the ERS-1 scatterometer wind pdfs are shown. The data is reprocessed with CMOD7.a with HOC corrections from ERS applied on top of the ASCAT HOC corrections (named CMOD7.e). The WVC dependency is reduced by the HOC corrections but is still present for low incidence angles (WVC numbers 1 and 2).

In Figure 8c) the NWP wind pdfs are shown.

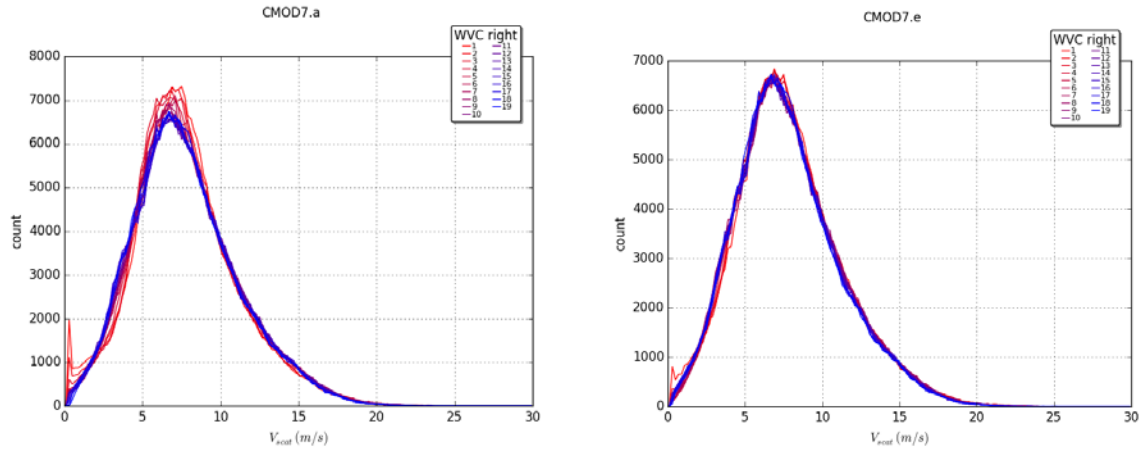

a) b)

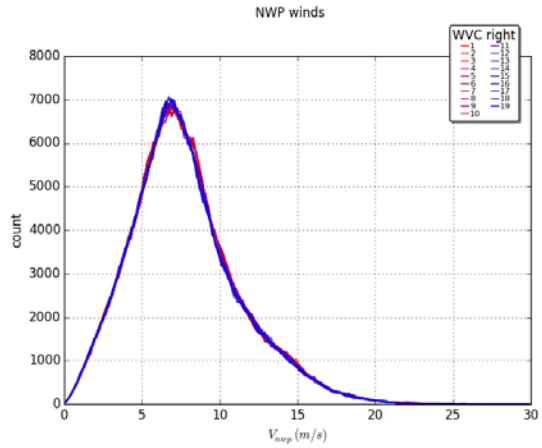

c)

Figure 8 - wind speed pdf from ERS-1 reprocessed data from 1995-01, ERA-interim stress equivalent winds

a) scattometer winds, CMOD7.a (with HOC corrections from ASCAT)

b) scattometer winds, CMOD7.e (CMOD7a with HOC corrections from ERS on top of the ASCAT HOC corrections)

c) NWP winds

In Figure 9 the wind speed and wind direction bias per WVC (scatterometer-NWP) are shown as well as their standard deviations.

Figure 9a) shows the biases for data reprocessed with CMOD7 with HOC corrections from ASCAT

Figure 9b) shows the biases for data reprocessed with CMOD7 and with HOC corrections from ERS on top of it.

Wind speed biases do not vary much and the standard deviations show a slight improvement when ERS HOC corrections are applied. The HOC benefits in wind direction SD are encouraging.

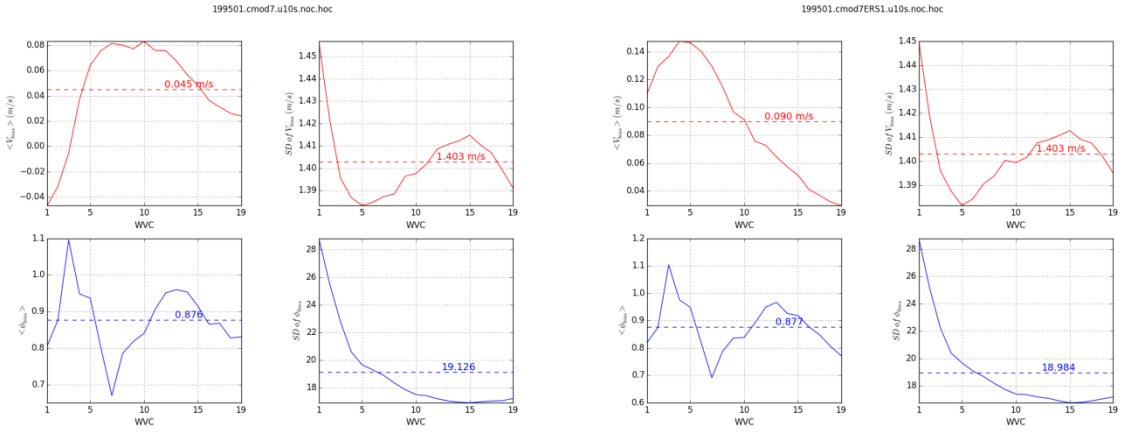

a) b)

Figure 9 - wind biases (scatterometer-NWP) per WVC for ERS-1 reprocessed data from 1995-01, ERA-interim model stress equivalent winds

a) CMOD7.a (with HOC corrections from ASCAT)

b) CMOD7.e (with HOC corrections from ERS on top of the ASCAT HOC corrections)

4 A consistent GMF for ERS and ASCAT (CMOD7.ae)

The CMOD7.a and CMOD7.e GMFs are combined into a new GMF CMOD7.ae, that is valid for both ASCAT and ERS incidence angle ranges. This is done by a linear interpolation in the incidence angle interval between 27° and 37°, the same interval as used for the interpolation between CMOD6 and C2013. Above 37° CMOD7.a is used, below 27° CMOD7.e. The linear interpolation guarantees a smooth transition.

Figure 10 shows the scatterometer wind speed pdfs from ASCAT and ERS after reprocessing with CMOD7.ae. Compared with previous results from CMOD7.a (see Figure 5b) and CMOD7.e (see Figure 8b) respectively, the differences are hard to detect by eye.

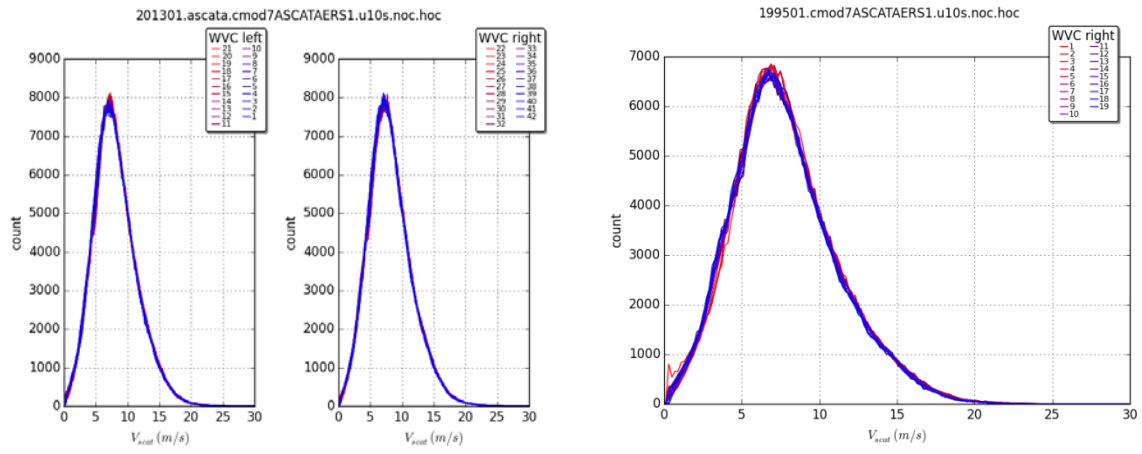

a) b)

Figure 10 - wind speed pdf from reprocessed data with, ERA-interim stress equivalent NWP winds and CMOD7.ae, including the HOC corrections from both ASCAT and ERS

a) ASCAT-A data from 2013-01

b) ERS-1 data from 1995-01

Wind bias differences are also small compared with the previous results, 0.160 m/s versus 0.154 m/s for ASCAT CMOD7.ae versus CMOD7.a, and 0.083 m/s versus 0.045 m/s for ERS CMOD7.ae versus

CMOD7.e. Also other statistics like MLE and wind speed standard deviations are similar. More of these results will be shown later on in this document.

5 Wind speed bias consistency

In AWDP wind processing NWP ocean calibration (NOC) is used to correct for small deviations of various origin. Typically the deviations show a wiggly pattern as function of incidence angle or WVC. The source of the deviations may be antenna calibration issues, GMF errors, or errors in the incidence angle derivation. NOC corrects for these errors by applying a correction to the sigma0 as a function of WVC and antenna. NOC has a direct effect on the wind speed bias versus WVC.

Differences in NWP data sets that are used also have a direct effect on the wind speed bias.

For OSI SAF near real time operational wind processing of ERS and ASCAT, real 10 m winds from the ECMWF operational model are used. For reprocessing of ERS and ASCAT for climatological purposes, stress equivalent 10 m winds from the ECMWF ERA-interim re-analysis are used.

Real 10 m winds and stress-equivalent winds have a bias of 0.2 m/s with respect to each other when averaged over the global oceans. Stress-equivalent winds have no global bias when compared to NWP equivalent neutral winds, but a regionally-dependent bias. CMOD5.n and later GMF versions yield stress-equivalent scatterometer winds, so these GMFs inherently give a global bias when compared with real NWP winds. This bias is taken into account where applicable.

The operational ECMWF archive contains wind at a high resolution. For ASCAT near real time operational processing ECMWF wind data on a ~ 16 km grid were used. On the other hand, the ERA-interim winds are only available on a grid of ~ 78 km but have the advantage that they are available and rather consistent over a long period, thus ideal for use in climatological data records and for use in ERS/ASCAT reprocessing as a reference. Operational and ERA-interim NWP wind data sets have a bias with respect to each other due to the differences in resolution and NWP model version.

The ERS WVC-dependent linear calibration is determined based on the operational ECMWF model and NWP ocean calibration (NOC), since it is used for the well-established ASCAT calibration procedure in operations. The difference between the operational and ERA-interim NOC for ASCAT is used to adapt the ERS NOC to the level of the ASCAT calibration (based on operations). After appropriate linear calibration by such amended NOC, the ERS and ASCAT wind pdfs should be similar.

In Figure 11 the NOC residuals from ASCAT-A data are shown with stress-equivalent NWP winds from the operational archive, stress-equivalent NWP winds from the ERA-interim archive, and with real NWP winds from the operational archive. In the latter case 0.2 m/s is added to the NWP winds in order to correct for the mean bias between real winds and neutral/stress-equivalent winds.

Figure 12 shows the differences between any combination of those three cases. In Figure 12a) and c) the incidence angle domain is stretched to include the ERS incidence angle domain also. The second-order polynomial fit from Figure 12a) (a_i =(3.54016444e-02, -4.52214853e-03, 3.33318404e-05)) is

used to compensate the wind speed bias that arise from using ERA-interim NWP winds instead of operational NWP winds for ERS reprocessing.

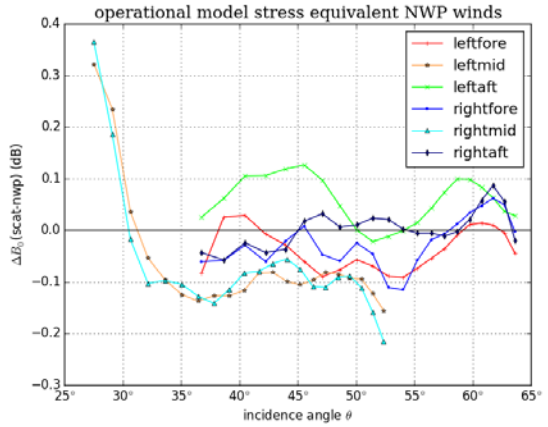

a)

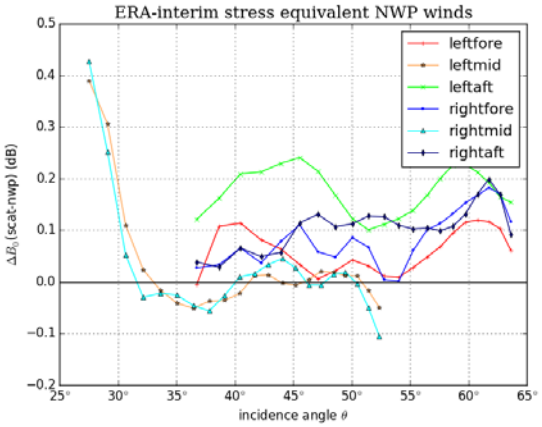

b)

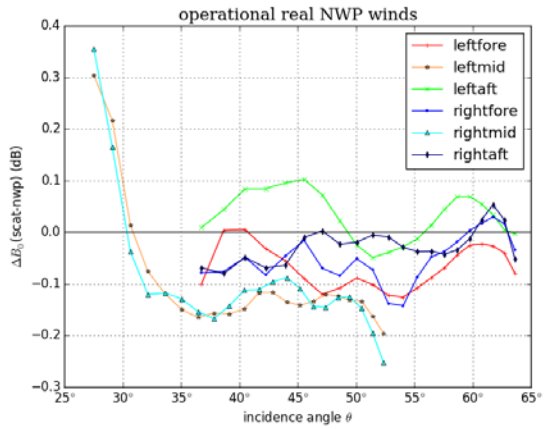

c)

Figure 11 – NOC residuals for ASCAT-A 2013 data reprocessed with CMOD7.ae and

a) operational stress equivalent NWP winds

b) ERA interim stress equivalent NWP winds

c) operational real NWP winds (with 0.2 m/s correction added)

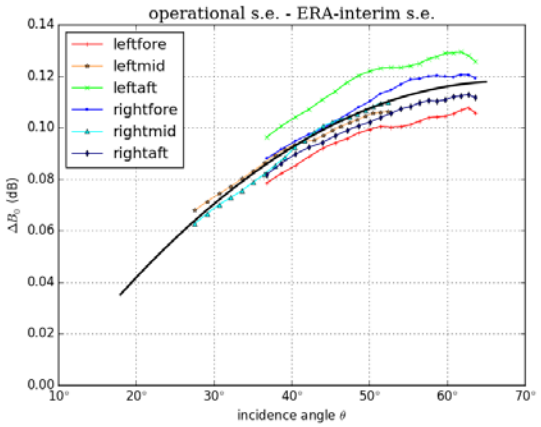

a)

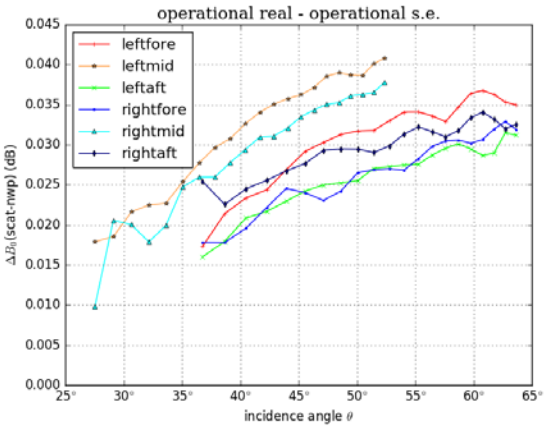

b)

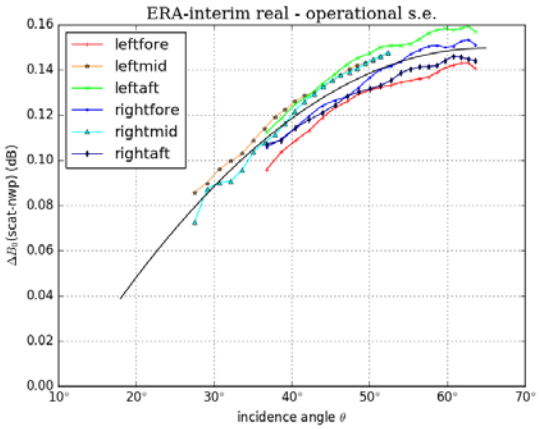

c)

Figure 12 – Double difference of NOC residuals from Figure 11

a) ERA-interim stress-equivalent NWP winds versus operational NWP stress-equivalent winds (b-a) , with polynomial fit;

b) operational stress-equivalent NWP winds versus operational real NWP winds (a-c);

c) ERA-interim stress-equivalent NWP winds versus operational real NWP winds (b-c), with polynomial fit.

In order to test the effect of the polynomial correction one month of data is reprocessed with ERA-interim stress-equivalent winds with and without the polynomial correction (Figure 13b and Figure 13a) and with operational stress-equivalent winds (Figure 13c). Indeed the wind speed biases of Figure 13b and Figure 13c are close together, because they use a similar NOC correction table, derived from the operational stress-equivalent winds (Figure 11a), where the polynomial correction compensates for the bias caused by the low-resolution ERA-interim NWP winds. The small remaining difference in bias is caused by the fact that the polynomial fit is an approximation for the NWP-dependent residuals, and because the polynomial fit is derived from a different period (the full year 2013). The difference in bias between Figure 13b and Figure 13a can be ascribed to the small data set.

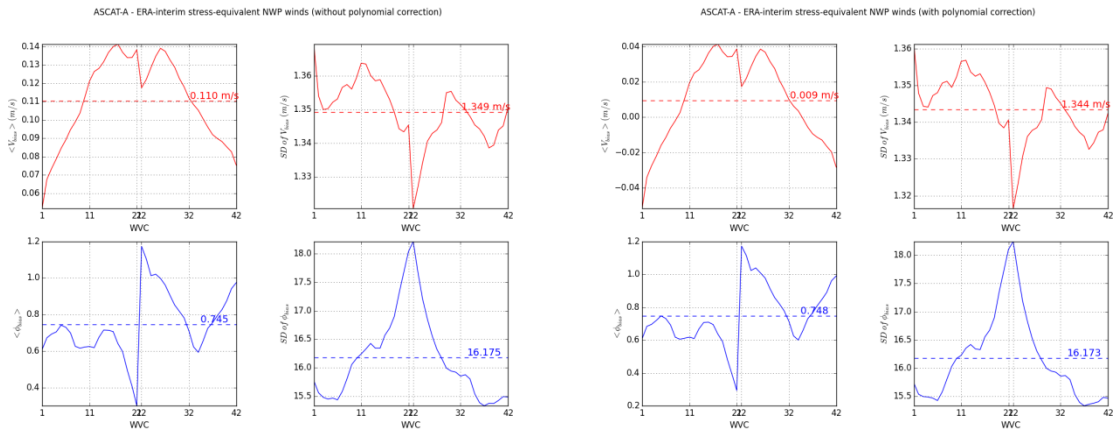

a)

b)

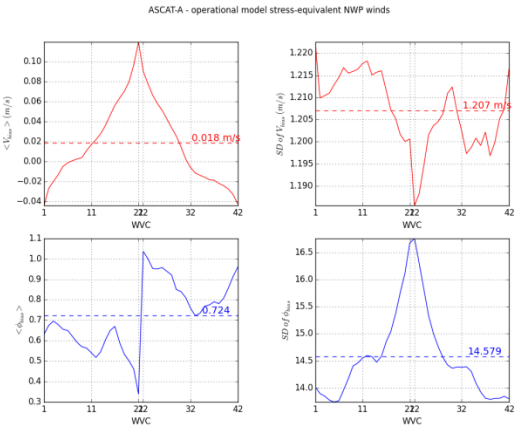

c)

Figure 13 – Wind biases from ASCAT-A 2013-01 reprocessed data

a) ERA-interim stress-equivalent NWP winds, no polynomial fit correction;

b) ERA-interim stress-equivalent NWP winds, with polynomial fit correction;

c) Operational stress equivalent NWP winds.

6 Wind, MLE and QC statistics (CMOD7.ae)

Below are several plots showing results from the wind statistics, Maximum Likelihood Estimate (MLE) statistics and Quality Control (QC) statistics from ASCAT-A and ERS-1 data reprocessed with CMOD7.ae. ASCAT is reprocessed with both operational model and ERA-interim model stress-equivalent winds. ERS is reprocessed with ERA-interim stress-equivalent winds only.

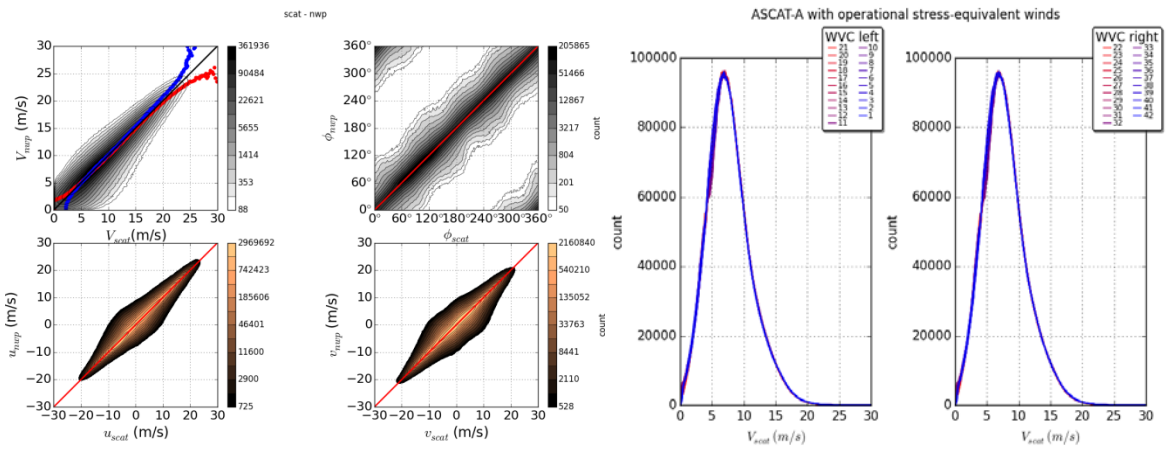

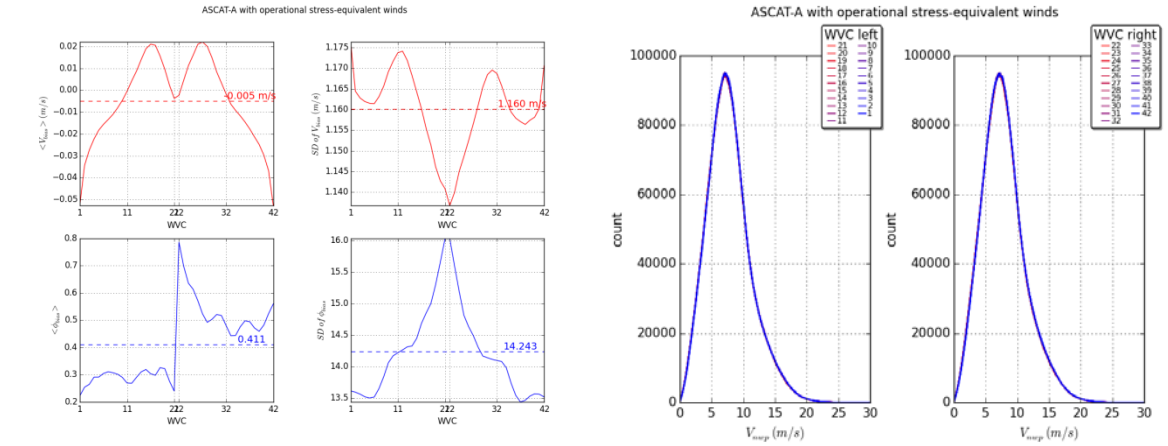

Figure 14 – Wind statistics of ASCAT-A data from 2013, reprocessed with CMOD7.ae, with operational model stress-equivalent winds:

a) Scatterometer-NWP histograms of the wind speed, wind direction, u-component, v-component;

b) Scatterometer wind pdfs as a function of WVC;

c) Wind speed and wind direction bias (scatterometer-NWP), and their standard deviation as a function of WVC;

d) NWP wind pdfs as a function of WVC.

In Figure 14a) histograms of ASCAT-A – NWP wind data are shown, Figure 14b) and d) show ASCAT-A and NWP wind speed pdfs respectively per WVC. In Figure 14c) the wind speed and wind direction biases and standard deviations are shown per WVC.

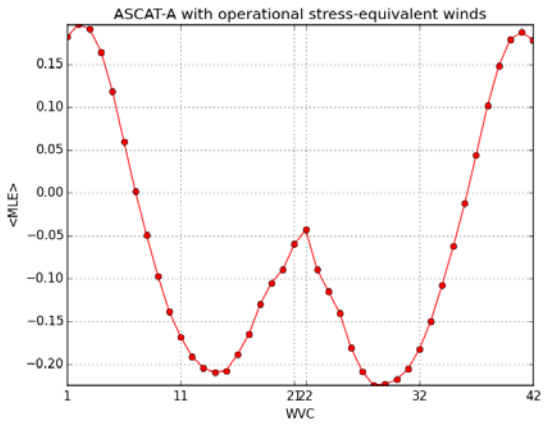

a)

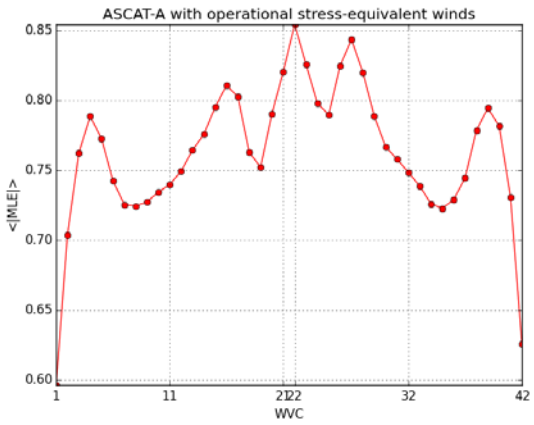

b)

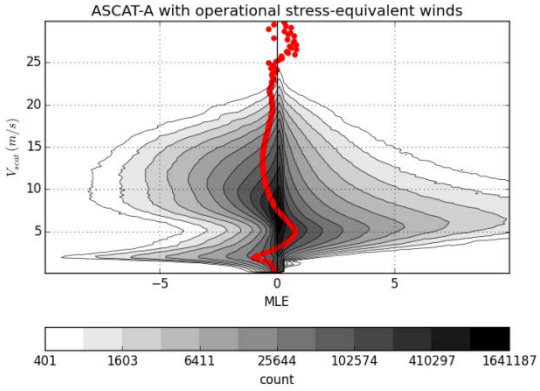

c)

Figure 15 – MLE or cone distance statistics from ASCAT-A data of 2013, reprocessed with CMOD7.ae, with operational model stress-equivalent winds:

a) <MLE> as a function of WVC;

b) <|MLE|> as a function of WVC;

c) contour plot of MLE as a function of scatterometer wind speed. In red the average value of the MLE is shown.

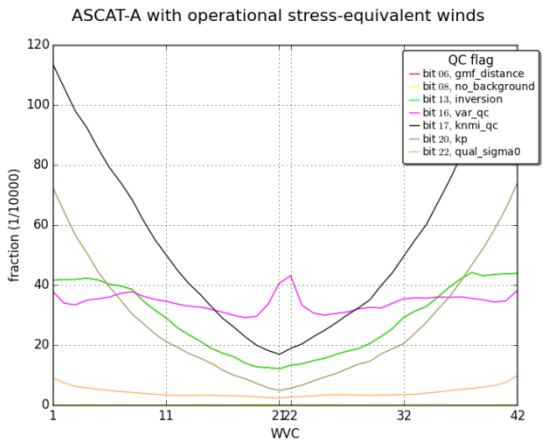

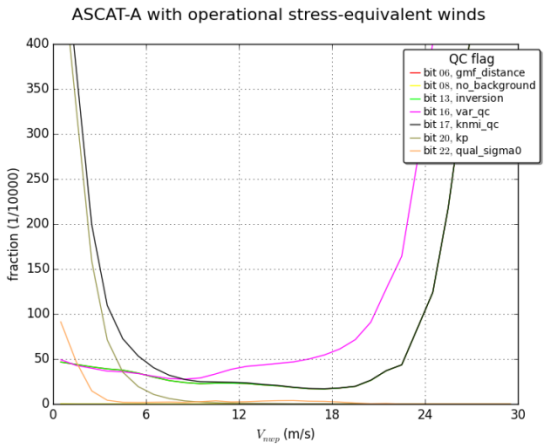

a) b)

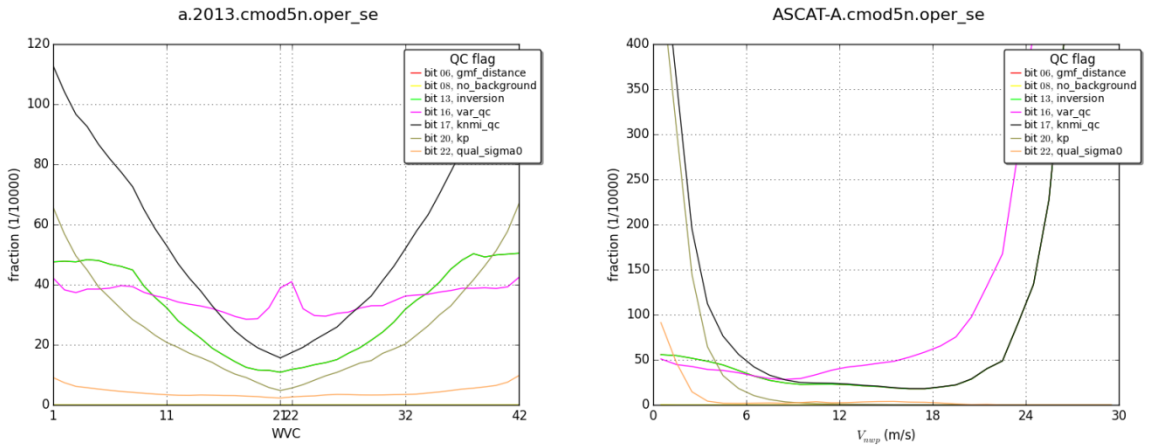

c) d)

Figure 16 – Quality Control statistics from ASCAT-A data of 2013, with operational model stress-equivalent winds

a) reprocessed with CMOD7.ae , QC flagged fraction as a function of WVC

b) reprocessed with CMOD7.ae, QC flagged fraction as a function of wind speed

c) reprocessed with CMOD5.n , QC flagged fraction as a function of WVC

d) reprocessed with CMOD5.n, QC flagged fraction as a function of wind speed

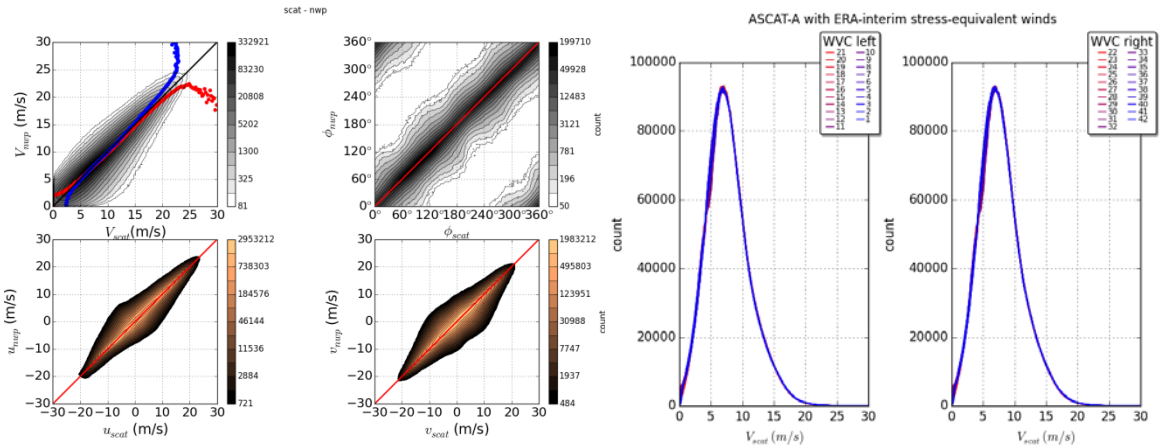

a) b)

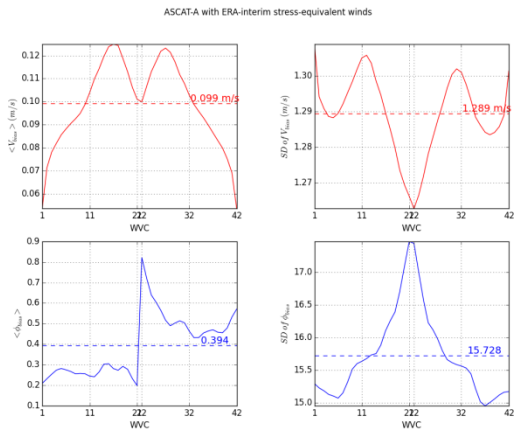

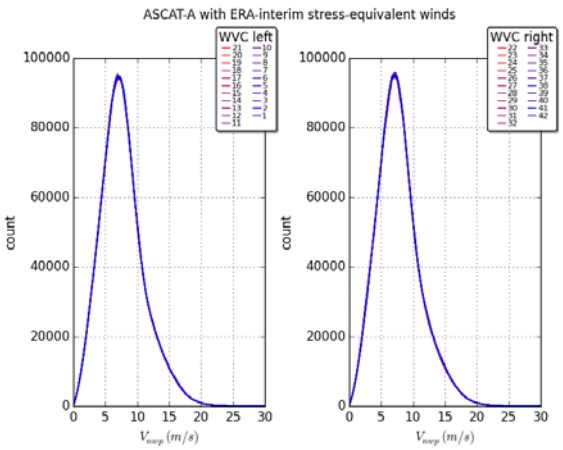

c) d)

Figure 17 – wind statistics from ASCAT-A data of 2013, reprocessed with CMOD7.ae, with ERA-interim model stress-equivalent winds:

a) Scatterometer-NWP histograms of the wind speed, wind direction, u-component, v-component;

b) Scatterometer wind pdfs as a function of WVC;

c) Wind speed and wind direction bias (scatterometer-NWP), and their standard deviation as a function of WVC;

d) NWP wind pdfs as a function of WVC.

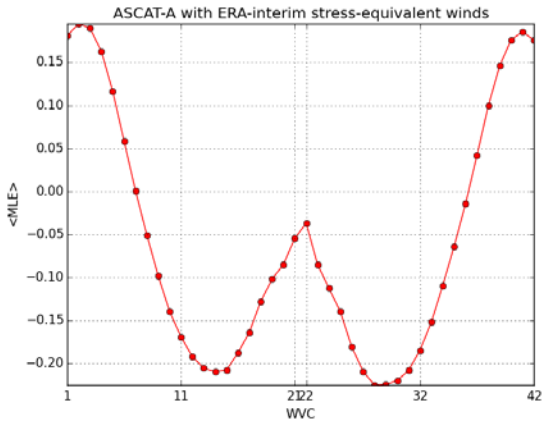

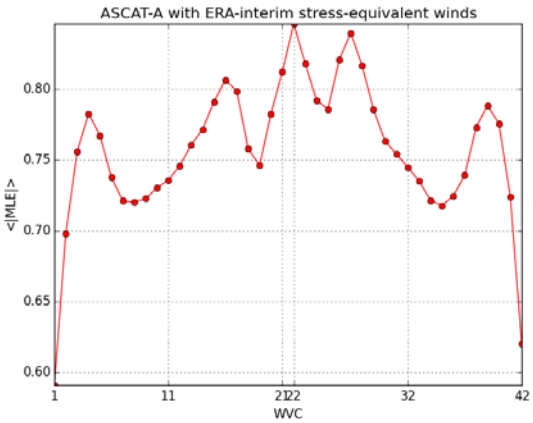

a) b)

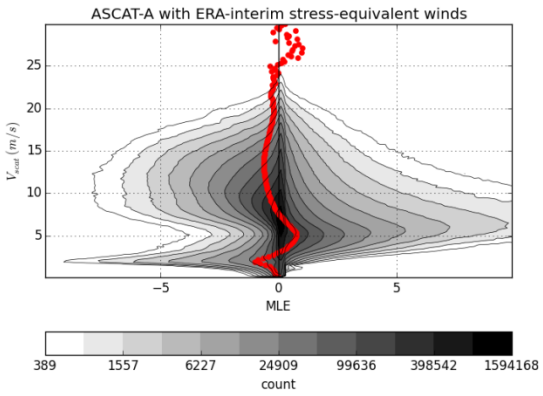

c)

Figure 18 – MLE or cone distance statistics from ASCAT-A data of 2013, reprocessed with CMOD7.ae, with ERA-interim model stress-equivalent winds:

a) <MLE> as a function of WVC

b) <|MLE|> as a function of WVC

c) Contour plot of MLE as a function of scatterometer wind speed. In red the average value of the MLE is shown

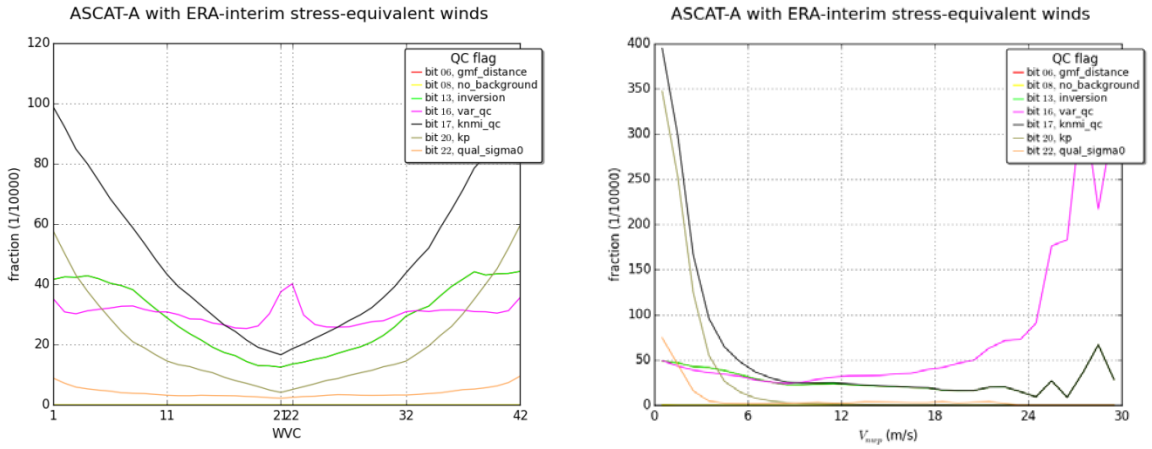

a) b)

Figure 19 – Quality Control statistics from ASCAT-A data of 2013, reprocessed with CMOD7.ae, with ERA-interim model stress-equivalent winds:

a) QC flagged fraction as a function of WVC;

b) QC flagged fraction as a function of wind speed.

Figure 17, Figure 18 and Figure 19 are analogous to Figure 14, Figure 15 and Figure 16 respectively but with ERA-interim background winds instead of operational model background winds.

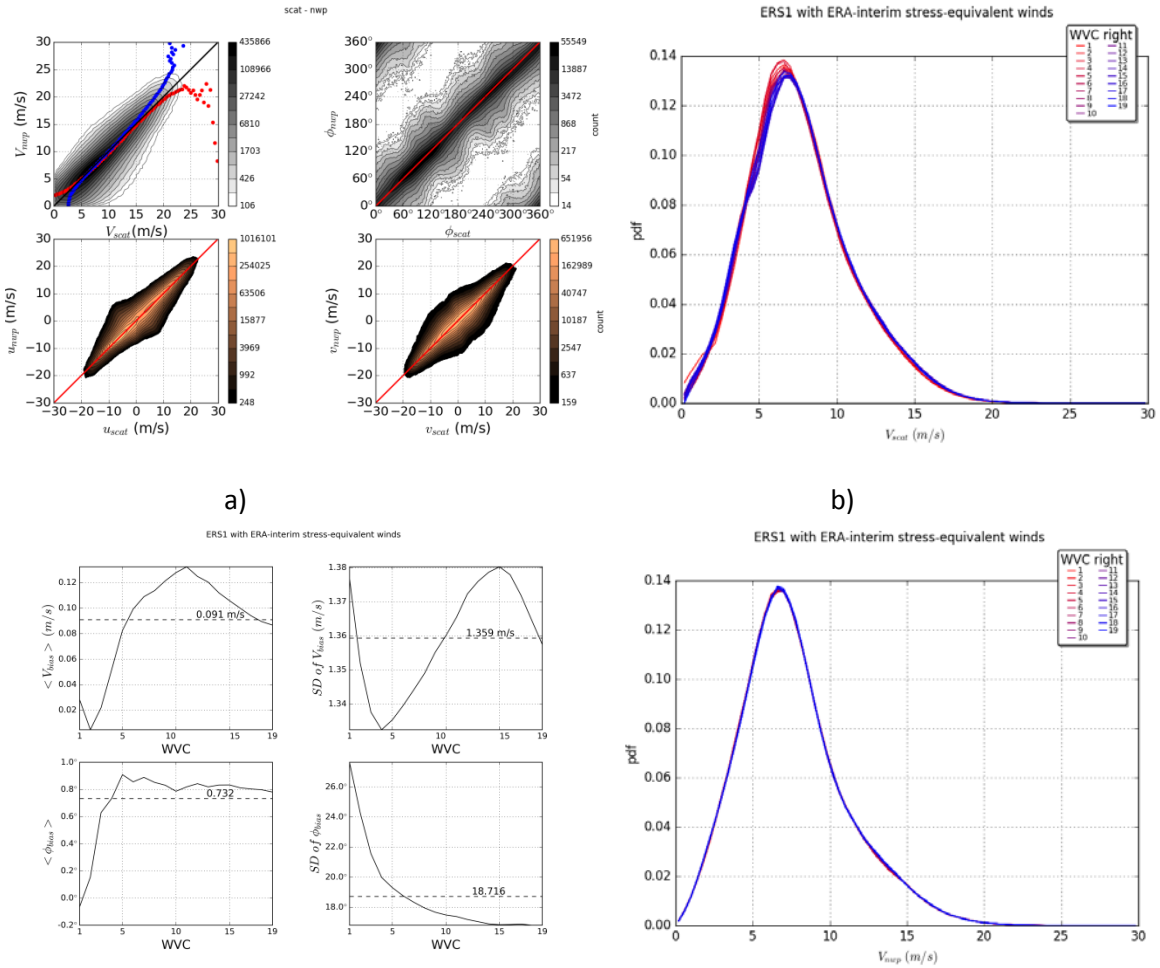

Figure 20 – Wind statistics from ERS-1 data of 1995, reprocessed with CMOD7.ae, with ERA-interim model stress-equivalent winds:

a) Scatterometer-NWP histograms of the wind speed, wind direction, u-component, v-component;

b) Scatterometer wind pdfs as a function of WVC;

c) Wind speed and wind direction bias (scatterometer-NWP), and their standard deviation as a function of WVC;

d) NWP wind pdfs as a function of WVC.

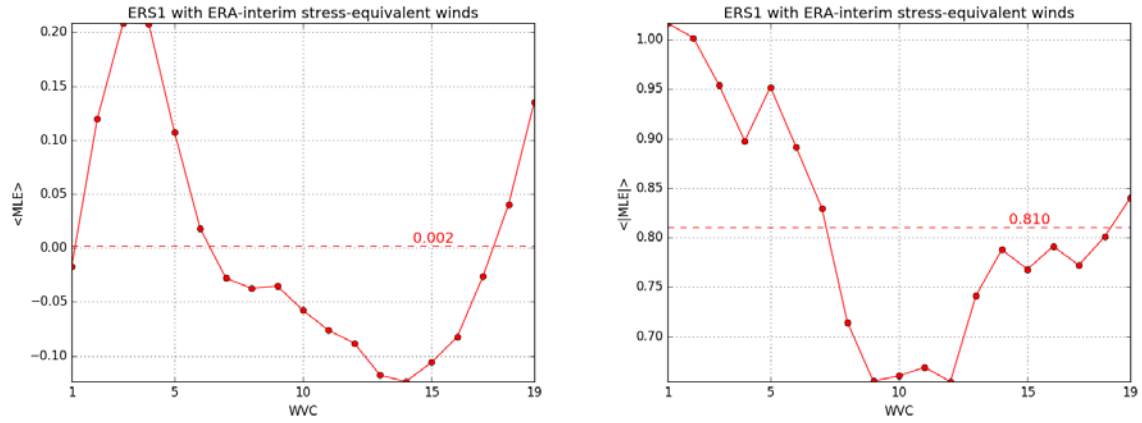

a) b)

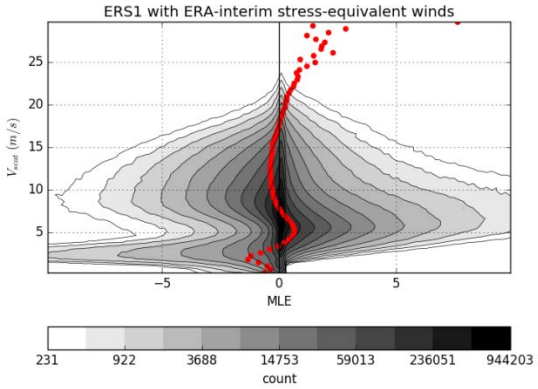

c)

Figure 21 – MLE or cone distance statistics from ERS-1 data of 1995, reprocessed with CMOD7.ae, with ERA-interim model stress-equivalent winds

a) <MLE> as a function of WVC;

b) <|MLE|> as a function of WVC;

c) Contour plot of MLE as a function of scatterometer wind speed. In red the average value of the MLE is shown.

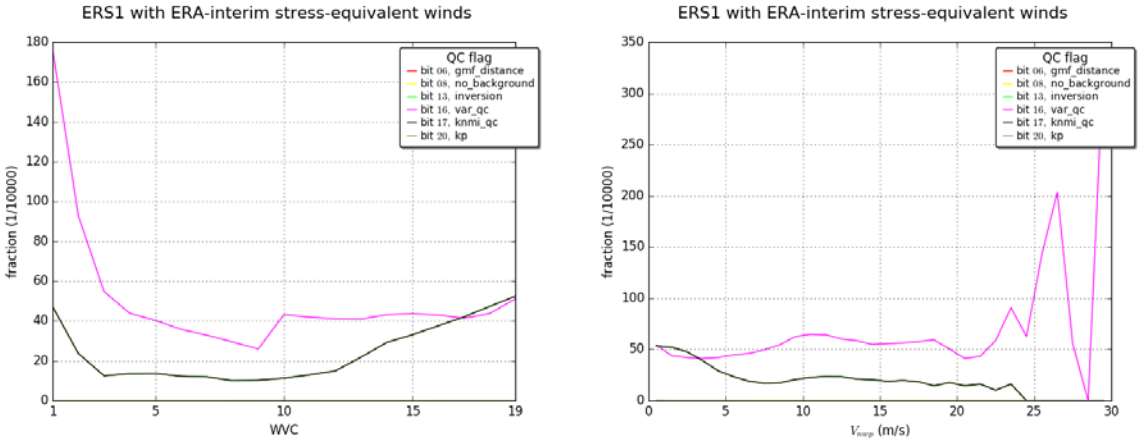

a) b)

Figure 22 - Quality Control statistics from ERS-1 data of 1995, reprocessed with CMOD7.ae, with ERA-interim model stress-equivalent winds:

a) QC flagged fraction as a function of WVC;

b) QC flagged fraction as a function of wind speed.

Figure 20, Figure 21 and Figure 22 are analogous to Figure 17, Figure 18 and Figure 19 respectively but with ERS-1 winds instead of ASCAT-A winds.

All results are within expectations.

7 Triple collocation validation

In this section, scatterometer wind data are compared with in situ buoy wind measurements. The buoy winds are distributed through the Global Telecommunication System (GTS) and have been retrieved from the ECMWF MARS archive. The buoy data are quality controlled and (if necessary) blacklisted by ECMWF [Bidlot et al., 2002]. We used a set of approximately 150 moored non-coastal buoys spread over the oceans (most of them in the tropical oceans and near Europe and North America) which are also used in the buoy validations that are routinely performed for the OSI SAF wind products (see the links on http://www.knmi.nl/scatterometer/osisaf/). Most of these buoys are located more than 50 km off the coast.

See Figure 23 for the locations of the buoys used in the comparisons. A scatterometer wind and a buoy wind measurement are considered to be collocated if the distance between the WVC centre and the buoy location is less than the WVC spacing divided by √2 and if the acquisition time difference is less than 30 minutes.

The buoy winds are measured hourly by averaging the wind speed and direction over 10 minutes. The real winds at a given anemometer height have been converted to 10 m equivalent-neutral winds using the LKB model [Liu et al., 1979] in order to enable a good comparison with the 10 m scatterometer stress-equivalent winds.

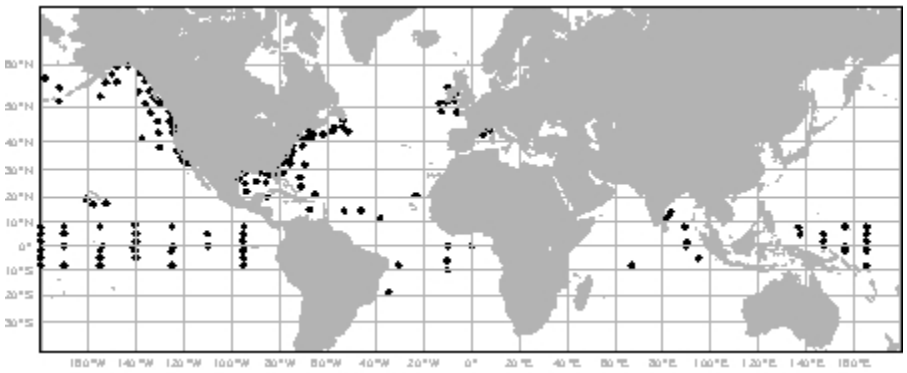

Figure 23 – Locations of the moored buoys used in the comparisons.

A triple collocation study was performed to assess the errors of the ASCAT, ECMWF and buoy winds independently. The triple collocation method was introduced by [Stoffelen 1998]. Given a set of triplets of collocated measurements and assuming linear calibration, it is possible to simultaneously calculate the errors in the measurements and the relative calibration coefficients. The triple collocation method can give the measurement errors from the coarse resolution NWP model perspective or from the intermediate resolution scatterometer perspective and from the fine resolution buoy perspective with further assumptions on the local buoy measurement error. A sub-WVC wind signal present in the buoy measurements, but not in the scatterometer winds is

attributed as buoy error on the scatterometer scale (representativeness error). This matter is introduced in [Stoffelen 1998] and extensively discussed in [Vogelzang et al. 2011].

Below are several tables showing results from the triple collocation of scatterometer winds, NWP winds and buoy winds for CMOD7.ae and ERS-1 (1994-1995), ASCAT-A/ASCAT-B (2013). The errors are with respect to the scatterometer, so the representation error, calculated from the difference between scatterometer and ECMWF spectra, is added to the ECMWF background errors and subtracted from the buoy and scatterometer errors.

Table 1 - Errors in u and v components (in m/s) with respect to the scatterometer scale

				Buoys		*Scatterometer*		*ECMWF*	
Scatterometer	Grid (km)	GMF	Background	σ_u (m/s)	σ_v (m/s)	σ_u (m/s)	σ_v (m/s)	σ_u (m/s)	σ_v (m/s)
ASCAT-A	25.0	CMOD5n	operational	1.17	1.26	0.54	0.71	1.30	1.36
ASCAT-A	25.0	CMOD7	operational	1.15	1.25	0.49	0.60	1.32	1.37
ASCAT-B	25.0	CMOD7	operational	1.18	1.25	0.46	0.57	1.31	1.36
ASCAT-A	12.5	CMOD7	operational	1.08	1.16	0.61	0.75	1.40	1.45
ASCAT-B	12.5	CMOD7	operational	1.10	1.14	0.56	0.73	1.40	1.45
ASCAT-A	25.0	CMOD7	ERA-interim	1.14	1.23	0.44	0.56	1.53	1.59
ERS-1	25.0	CMOD7	ERA-interim	1.36	1.42	0.62	0.88	1.39	1.51

In Table 1 the standard deviation σ is shown of the *u* and *v* wind components for several scatterometer products. In the first two rows the same datasets reprocessed with CMOD5.n and CMOD7 are compared. For CMOD7 the scatterometer standard deviations are smaller than for CMOD5.n thus the wind product is improved with the use of CMOD7. Standard deviations of ASCAT-A and ASCAT-B are close together. ERS-1 has a somewhat higher standard deviation than ASCAT-A and ASCAT-B. Standard deviations for the coastal product (12.5 km grid size) are higher than for the corresponding 25.0 km grid size product, as is to be expected due to the lower signal to noise ratio. Note, however, that the buoy errors are smallest for the 12.5-km products, since these are the closest to the buoy resolution. Conversely, due to their smoothness, the ECMWF winds show higher error for the 12.5-km products than for the 25-km products. As anticipated, ERA-interim errors are larger than operational ECMWF wind errors. Note that the buoy and scatterometer errors are relatively high and the ERA-interim error relatively low for ERS, indicating that it has both poorer accuracy and resolution than the equivalent ASCAT products.

From the triple collocation analysis, we can also determine the calibration of the scatterometer and NWP winds relative to the buoy winds. The calibration coefficients *a* and *b* relate the uncalibrated scatterometer wind components (u_{unc}, v_{unc}) to the "true" wind components (u_{cal}, v_{cal}) according to:

$$\begin{aligned} u_{cal} &= a_u u_{unc} + b_u \\ v_{cal} &= a_v v_{unc} + b_v \end{aligned} \quad , \qquad (1)$$

Table 2 - Calibration coefficients (u and v components, in m/s) with respect to buoys

			SCAT				BACK			
instrument	background	grid	b_u	b_v	a_u	a_v	b_u	b_v	a_u	a_v
ASCAT-A	operational	25.0	-0.03	0.04	0.986	1.001	-0.15	0.00	0.999	1.037
ASCAT-B	operational	25.0	-0.04	0.05	0.983	1.000	-0.15	0.00	0.998	1.034
ASCAT-A	operational	12.5	-0.02	0.04	0.995	1.015	-0.16	0.00	1.004	1.035
ASCAT-B	operational	12.5	-0.02	0.05	0.986	1.008	-0.15	-0.00	1.004	1.034
ASCAT-A	ERA-interim	25.0	-0.05	0.02	0.999	1.019	-0.15	-0.04	1.015	1.060
ERS-1	ERA-interim	25.0	-0.12	-0.04	0.989	1.018	-0.29	-0.15	0.980	0.984
precision			0.01	0.01	0.001	0.002	0.01	0.01	0.001	0.001

In Table 2 the calibration coefficients derived from the triple collocation are shown. We note that the b coefficients are generally small and may be ignored, i.e., the b-coefficient is fixed to zero. If we further require the u and v scaling to be identical, then a wind speed scaling would emerge. In Table 3 the a-coefficient for such wind speed scaling is shown.

Table 3 - Calibration coefficients (wind speed only) with respect to buoys

			SCAT	BACK
instrument	background	grid	$a_u = a_v$	$a_u = a_v$
ASCAT-A	operational	25.0	0.994	1.019
ASCAT-B	operational	25.0	0.992	1.017
ASCAT-A	operational	12.5	1.005	1.021
ASCAT-B	operational	12.5	0.997	1.019
ASCAT-A	ERA-interim	25.0	1.009	1.038
ERS-1	ERA-interim	25.0	0.978	0.992
precision			0.001	0.001

The calibration coefficients do not deviate too much from their ideal values (a=1, b=0) so no further correction is needed with these results.

8 Discussion

A higher-order calibration (HOC) correction is applied which matches the scatterometer wind pdf for each WVC to a predefined wind speed pdf. The predefined wind speed pdf is a combination of a theoretical function with fitted parameters on the ascending side, and a mean scatterometer pdf on the descending side. The HOC largely reduces the WVC-dependency of the wind speed pdf and also reduces the local maxima in the wind speed pdf.

Wind speed biases for the various scatterometer products, ERS-1, ASCAT-A and ASCAT-B (for 25 km WVC size and for the coastal product of 12.5 km WVC size) with respect to NWP stress-equivalent wind are compared to each other. NWP Ocean Calibration (NOC) is applied for ASCAT (using operational EWMF stress-equivalent winds) and for ERS (using ERA-interim stress-equivalent winds). Difference in bias caused by these differences in used NWP wind field and differences in the ECMWF model software version, are compensated for.

The resulting CMOD7 shows good results on all relevant parameters, wind speed and direction, wind speed bias, cone distance and quality control rejection rate for both ERS and ASCAT scatterometers. Triple collocation with NWP and buoy winds also show good results so there is no need to apply further calibration coefficients to the data.

In the ESA SCIROCCO project, a noise floor correction is being developed for the ERS-1 and ERS-2 scatterometers. The necessary corrections are especially large for ERS-2. This is the reason that we have only used ERS-1 data here. In future the noise floor correction will be applied to ERS data. A first test on ERS-1 indicated that the effect on overall statistics is only small. Also, an interpolation for HOC corrections to the lower ERS mid beam incidence angles (18^{o}-25^{o}) may be performed in future.

Glossary

ASCAT	- Advanced SCATterometer
AWDP	- ASCAT Wind Data Processor
CMOD	- C-band geophysical model function used for ERS and ASCAT
ECMWF	- European Centre for Medium-Range Weather Forecasts
ERS	- European Remote Sensing scatterometer
MLE	- Maximum Likelihood Estimate
NOC	- NWP Ocean Calibration
NWP	- Numerical Weather Prediction
pdf	- probability distribution function
WVC	- Wind Vector Cell

References

[Bidlot et al, 2002] Bidlot J., D. Holmes, P. Wittmann, R. Lalbeharry, and H. Chen, Intercomparison of the performance of operational ocean wave forecasting systems with buoy data, Wea. Forecasting, vol. 17, 287-310, 2002

[Liu et al, 1979] Liu, W.T., K.B. Katsaros, and J.A. Businger, Bulk parameterization of air-sea exchanges of heat and water vapor including the molecular constraints in the interface, J. Atmos. Sci., vol. 36, 1979.

[Ricciardulli, 2014] Lucrezia Ricciardulli and Frank Wentz, Progress and future plans on an ocean wind vector wind climate record. Products from OCEANSAT-2 Scatterometer, International Ocean Vector Wind Science Team Meeting, June 2014, Brest, France, http://coaps.fsu.edu/scatterometry/meeting/docs/2014/ClimateDataRecord/Ricciardulli_ovwst_2014_CDR_posted.pdf

[Stoffelen and Anderson, 1997] Stoffelen, Ad, and David Anderson, "Scatterometer Data Interpretation: Measurement Space and inversion", J. Atm. and Ocean Techn., 14(6), 1298-1313, 1997.

[Stoffelen, 1998] Stoffelen, A., Toward the true near-surface wind speed: error modelling and calibration using triple collocation, J. Geophys. Res. 103C4, 7755-7766, 1998.

[Verspeek, 2012] J. Verspeek et al (2012) "Improved ASCAT Wind Retrieval Using NWP Ocean Calibration", IEEE Transactions on Geoscience and Remote Sensing, vol 50, pp 2488 - 2494, doi: 10.1109/TGRS.2011.2180730.

[Verspeek, 2015] J. Verspeek and A. Stoffelen, "CMOD7", OSI SAF technical report, SAF/OSI/CDOP2/KNMI/TEC/RP/237, 2015

[Vogelzang et al, 2011] Vogelzang, J., A. Stoffelen, A. Verhoef, and J. Figa-Saldaña (2011), On the quality of high-resolution scatterometer winds, J. Geophys. Res., 116, C10033, doi:10.1029/2010JC006640.

[Vogelzang and Stoffelen, 2016] J. Vogelzang and A. Stoffelen, 2016: "Ascat calibration", NWPSAF report NWP-KN-TR-???, KNMI, De Bilt, The Netherlands